Recent Developments In Computational Fracture Mechanics At Cardiff

B.L. Karihaloo and Q.Z. Xiao
School of Engineering, Cardiff University
Queen's Buildings, P. O. Box 925, Cardiff CF24 0YF, UK

ABSTRACT

The following most recent developments in computational fracture mechanics at Cardiff University are reviewed: hybrid crack element (HCE) which can give directly the stress intensity factor (SIF) as well as the coefficients of higher order terms in the plane linear elastic crack tip asymptotic field; extended finite element method (XFEM) which avoids using a mesh conforming with the crack as is the case with the traditional FEM and gives highly accurate crack tip fields; penalty function technique for handling point loads; and compressed sparse row (CSR) storage scheme for efficient implementation of the above techniques. Possible future improvements are also discussed.

Keywords: Extended finite element method (XFEM); Hybrid crack element (HCE); Penalty function; Point load; Sparsity storage; Statically admissible stress recovery (SAR)

1. INTRODUCTION

An overview of the most recent developments in computational fracture mechanics at Cardiff University is given.

First, the improvements of hybrid crack element (HCE), which was originally introduced by Tong et al. [1] for evaluating only the stress intensity factor (SIF), will be discussed. It has been extended so that now it is possible to determine accurately and directly (i.e. without the use of the energy related quantities like the *J*-integral, or other extra post-processing) the SIF as well as the coefficients of higher order terms in the plane linear elastic crack tip asymptotic fields [2, 3]. In a very recent development it has been further demonstrated that the HCE need not be a special element; it can be generated from any regular finite element (FE) mesh so that it can be included in any commercial FE code [4].

Second, the Cardiff contribution to the extended FE method (XFEM) [5-7] will be included. XFEM avoids using a mesh conforming with the crack as is the case with the traditional FEM. The standard local FE approximation around the crack is enriched with not only discontinuous Heaviside functions along the crack faces but also the asymptotic fields at nodes surrounding the crack tip using a partition of unity method (PUM). Our emphasis is on improving the accuracy of the crack tip fields. When the crack tip asymptotic field, e.g. Williams expansion, is available, the enriched approximation is enforced to be equivalent to this crack tip field [8, 9]. When the crack tip asymptotic field is not available and enrichment functions meet only the local displacement boundary conditions, a statically admissible stress recovery (SAR) method [10] is introduced. It uses basis functions, which meet the equilibrium condition within the domain and the local traction conditions on the exterior boundaries, and moving least-squares (MLS) to fit the stresses at sampling points (e.g., quadrature points) obtained by the FEM.

Third, a technique is introduced for handling point loads accurately. The displacement field in the neighbourhood of a point load is imposed as a constraint on the displacements at nodes

surrounding this point. These constraints are enforced through a penalty function approach. Accurate handling of point loads is especially important when the point load is close to the crack tip as in the evaluation of weight functions [11].

Fourth, the improvements to XFEM and to the accurate handling of point loads mean that the stiffness matrix can be very sparse, significantly increasing the bandwidth in the conventional skyline storage scheme. To avoid this, a compressed sparse row (CSR) storage scheme [12] is introduced. It stores only the row and column indices of each non-zero element together with its value. Addresses of the diagonal entries are also stored to simplify the retrieval of a specific element.

Finally, future directions of research will be indicated.

2. HYBRID CRACK ELEMENT (HCE)

A two dimensional (2D) n_d-node polygonal HCE is shown in Fig. 1a. If we ignore the body force and assume that no element boundary displacements have been prescribed, the HCE can be formulated from the following simplified variational functional [1, 2]

$$\Pi_m^e(u \text{ or } T, \tilde{u}) = \int_{S_\sigma^e} u^T (\frac{1}{2}T - \bar{T})ds - \int_{\partial\tilde{A}^e} (\frac{1}{2}u^T - \tilde{u}^T)T\, ds \qquad (1)$$

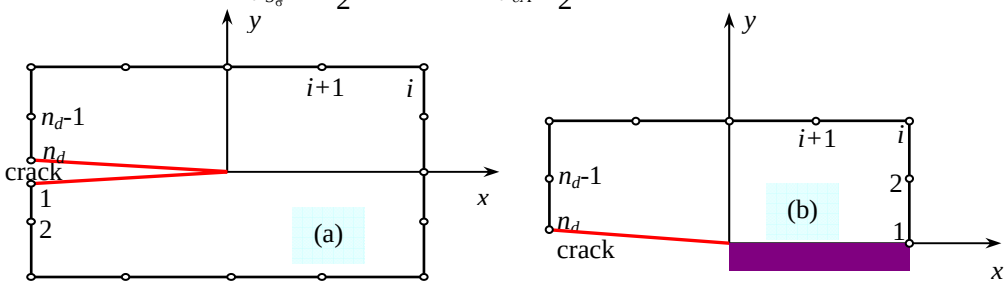

Fig. 1. An n_d-node polygonal HCE for a mixed mode (a) or pure *mode I* (or *II*) crack (b).

The tractions $\bar{T}_i$ are prescribed on the boundary segment S_σ^e; the interelement boundary $\partial\tilde{A}^e$ is common with the adjacent elements. Displacements u_i and tractions $T_i(=\sigma_{ij}n_j)$ are independent of the other elements and taken from the crack tip asymptotic expansions (i.e. Williams expansions) excluding rigid body and zero energy modes, but boundary displacements $\tilde{u}_i$ have to be the same for the two elements over their common boundaries $\partial\tilde{A}^e$. σ_{ij} denote stresses, and n_j are the direction cosines of the unit outward normal to ∂A^e. Subscripts i and j take the values 1 and 2, and the summation convention on repeated indices is used.

Three-point Gauss integration for each segment of $\partial\tilde{A}^e$ ensures good accuracy, since $\partial\tilde{A}^e$ is away from the crack tip, thus avoiding numerical integration of the singular integrand. Integrations on crack faces S_σ^e may be carried out analytically; if they are traction-free, as in most cases, the integrals vanish. The element must satisfy the following condition for stability

$$n_\beta \geq n_q - n_r \qquad (2)$$

where n_β and n_q (=$2n_d$) are the respective number of element stress and nodal displacement parameters employed, and n_r(=3 for 2D problems) the number of independent rigid body modes. If (2) becomes an equality, the best parameter matching condition is achieved.

If we restrict our attention to pure *mode I* (or *II*) crack problems, the half polygonal element with n_d nodes shown in Fig. 1b may be used for constructing the HCE by exploiting the symmetric (*mode I*) or asymmetric (*mode II*) conditions along the line of extension of the crack. We need only integrate along the outer boundary and avoid integrations along the line of extension of the crack.

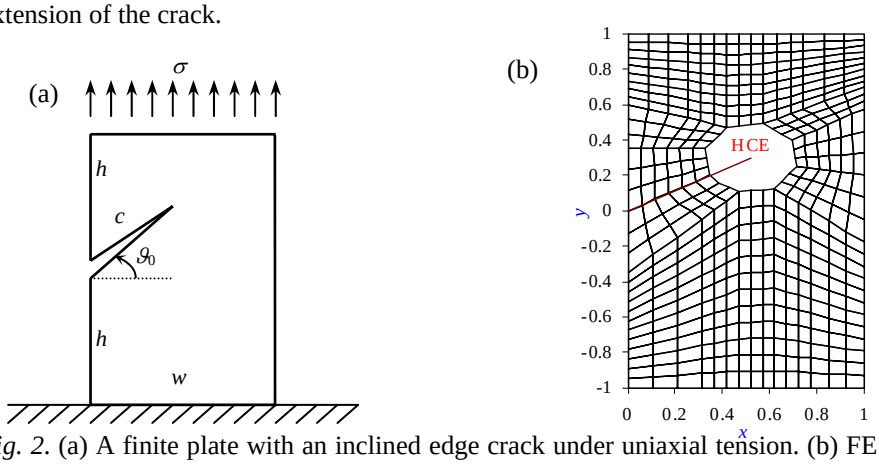

Fig. 2. (a) A finite plate with an inclined edge crack under uniaxial tension. (b) FE mesh with one 25-node HCE and 423 elements giving 487 nodes.

In the implementation of HCE in the literature [1-3], HCEs are first designed at each crack tip and then the whole domain is meshed taking into account the boundaries of the domain as well as the HCEs. An example solved by Xiao and Karihaloo [3] is shown in Fig. 2. This complicates the meshing task. A general FE mesh can actually be used by forming the HCE from elements surrounding the crack tip. An example is given in Fig. 3.

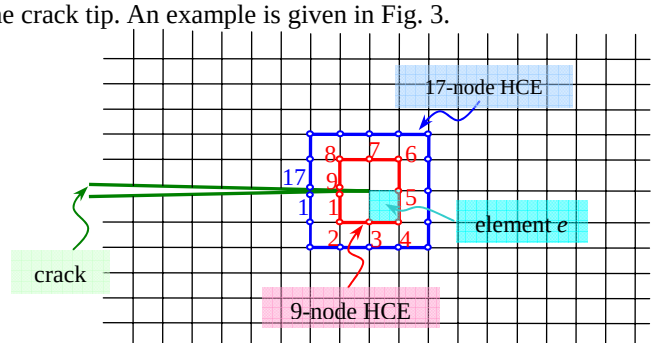

Fig. 3. Illustration of how 4-node quadrilateral elements of an existing FE mesh can be converted to an HCE with required number of nodes. The crack is lying along element boundaries.

The elements used for the formulation of the HCE will be skipped in the element analysis process, since their stiffness matrices are not required. The nodes lying inside the HCE are not actually used, and the corresponding degrees of freedom will result in zero pivots in the factorization process. This problem can be easily handled by changing these zero pivots to one and continuing the solution process, as in the HSL MA57 package. Fig. 4 shows an angle-cracked plate under tension studied by Karihaloo and Xiao [4]. The 4-node plane hybrid stress element PS of Pian and Sumihara [13] is used in conjunction with the HCE. 2×2 Gauss quadrature is employed for the formulation of PS. A state of plane stress is assumed and the thickness is assumed to be unity. Young's modulus $E = 1$, Poisson's ratio $\nu = 0.25$. All nodes on the bottom line are fixed in the vertical (y) direction, but just the extreme left point on

the line is fixed also in the horizontal (x) direction. The results for the right crack tip are shown in Table 1. The corresponding results for the left crack tip are almost the same. These results show that HCE constructed by the second-layer nodes around the crack tip, or, 4-node elements surrounding the element(s) including the tip, gives highly accurate SIFs and T-term.

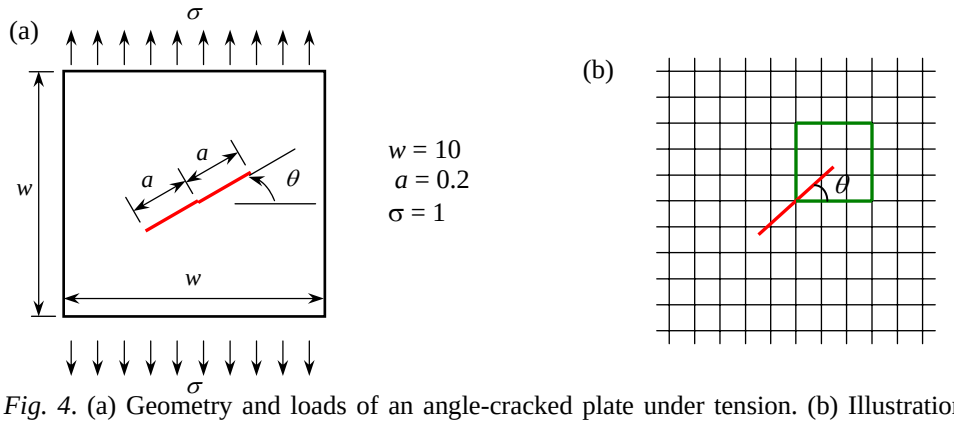

Fig. 4. (a) Geometry and loads of an angle-cracked plate under tension. (b) Illustration of the HCE for the right crack tip formed by the second-layer nodes around the crack tip, or, elements surrounding the element(s) including the tip, from a 100×100 uniform division of the plate.

Table 1. Coefficients of the Williams expansion for the right tip of the crack.

	Results of HCE					Exact solution	
θ	a_1	b_1	a_2	a_3	b_3	a_1	b_1
0	0.31580	0.00005	-0.25055	0.40183	-0.00011	0.31623	0
15	0.29412	-0.07879	-0.21632	0.37722	-0.10076	0.29504	-0.07906
30	0.23708	-0.13658	-0.12404	0.29589	-0.17232	0.23717	-0.13693
45	0.15822	-0.15773	-0.00246	0.20176	-0.20098	0.15811	-0.15811
60	0.07875	-0.13670	0.12487	0.10046	-0.17299	0.07906	-0.13693
75	0.02221	-0.07882	0.21695	0.02143	-0.09880	0.02118	-0.07906
90	0.00005	0.00001	0.24981	0.00032	-0.00004	0	0

3. EXTENDED FINITE ELEMENT METHOD (XFEM)

The original XFEM [5-7] (Fig. 5) used only the singular (leading) terms, and the additional coefficients at each enriched node are independent. It predicts accurate global displacements but SIFs at the crack tip have to be evaluated by a post-processing procedure. In order to improve the accuracy of local fields so as to determine the SIF directly, the FE approximation of the crack tip node as well as its surrounding nodes are enriched with not only the first term but also the higher order terms of the linear

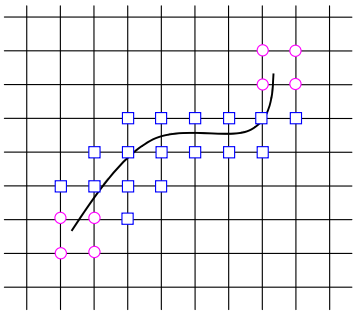

Fig. 5. A crack on a uniform mesh without consideration of the crack geometry. The squared nodes are enriched with the Heaviside function centred at the crack line whereas the circled nodes are enriched with the known crack tip fields.

elastic crack tip asymptotic field using the PUM [8, 9]. The approximation of displacements after enrichment becomes

$$\begin{Bmatrix} u^h(x) \\ v^h(x) \end{Bmatrix} = \sum_{i\in I} \phi_i(x) \begin{Bmatrix} u_{0i} \\ v_{0i} \end{Bmatrix} + \sum_{j\in J\cap I} \phi_j(x) H(x) \begin{Bmatrix} b_{1j} \\ b_{2j} \end{Bmatrix} + \sum_{m\in M_k\cap I} \phi_m(x) \sum_{n=1}^{N} \begin{bmatrix} f_{11n} & f_{12n} \\ f_{21n} & f_{22n} \end{bmatrix} \begin{Bmatrix} K_{Inm}^{(tip\,k)} \\ K_{IInm}^{(tip\,k)} \end{Bmatrix} \tag{3}$$

where I is the set of all nodes in the element, (u_{0i}, v_{0i}) are the regular degrees of freedom at node i, ϕ_i is the FE shape function associated with node i. J is the set of nodes whose support is intersected by the crack but do not cover any crack tips, the function $H(x)$ is the Heaviside function centred on the crack discontinuity, and (b_{1j}, b_{2j}) are the corresponding additional degrees of freedom. M_k is the set of nodes that are enriched around the crack tip k, which includes all nodes within a characteristic radius from crack tip k, in which the asymptotic fields dominate the solution. $K_{Inm}^{(tip\,k)}$ and $K_{IInm}^{(tip\,k)}$ are the coefficients, and f_{ijn} the angular functions.

We define the elements that include the crack tip k as the first-layer elements of the crack tip with enriched nodes. The nodes in the first-layer elements are defined as the first-layer enriched nodes and denoted by M_{k1}. The elements immediately adjacent to the first-layer elements are defined as the second-layer elements, and the nodes that are in the second-layer elements, but not in the first-layer elements, are defined as the second-layer enriched nodes. Additional layers of elements and enriched nodes can be defined in a similar manner. The additional coefficients $K_{Inm}^{(tip\,k)}$, $K_{IInm}^{(tip\,k)}$ for each order n at the first-layer enriched nodes of crack tip k, i.e., $m\in M_{k1}\cap I\equiv I$, are constrained to be equal through a penalty function approach. The third term on the right hand side of (3) becomes the actual crack tip asymptotic fields, and the additional coefficients are the relevant coefficients of the crack tip asymptotic fields. The additional coefficients at the other enriched nodes at the crack tips are assumed to be independent, thus ensuring a seamless link between the approximation matching the crack tip field and the standard FE approximation, using PUM. A penalty factor of 10^4E guarantees the convergence of numerical solutions.

Liu et al. [9] solved the plate with an inclined centre crack (Fig. 4a) with the XFEM. The parameters used are: W=10, a=0.5, σ=1, E=100 and ν=0.3. A 100×100 uniform division was used together with the 4-node plane isoparametric element Q4. The first 11 terms are retained in the asymptotic solution and three layers of enriched nodes around the crack tips are chosen. The numerical results listed in Table 2 show that without using a mesh conforming with the crack, high accuracy of the fields near the crack tip can be maintained and excellent agreement with the exact solution obtained for the entire range of θ.

Table 2. Results for K_I and K_{II} of an inclined centre crack in a plate under tension.

θ	XFEM		Exact Solution	
	K_I	K_{II}	K_I	K_{II}
0	1.271	0	1.253	0
5	1.263	0.110	1.244	0.109
10	1.238	0.213	1.216	0.214
15	1.194	0.312	1.169	0.313
20	1.126	0.404	1.107	0.403
25	1.047	0.480	1.029	0.480
30	0.960	0.551	0.940	0.543
35	0.853	0.592	0.841	0.589
40	0.745	0.620	0.735	0.617
45	0.625	0.645	0.627	0.627
50	0.520	0.622	0.518	0.617
55	0.392	0.585	0.412	0.589
60	0.288	0.539	0.313	0.543
65	0.197	0.471	0.224	0.480
70	0.144	0.400	0.147	0.403
75	0.084	0.312	0.084	0.313
80	0.036	0.216	0.038	0.214
85	0.009	0.108	0.010	0.109
90	0	0	0	0

4. STATICALLY ADMISSIBLE STRESS RECOVERY (SAR)

The method discussed above is only applicable when the crack tip asymptotic field is known. For most practical situations, the crack tip fields are not available. However, enrichment functions meeting the local displacement conditions adjacent to the crack tip can be chosen easily. In order to obtain accurate stresses, the SAR scheme is introduced.

The MLS interpolant $\sigma^h(x)$ of the stress $\sigma(x)$ is defined in the domain Ω by

$$\sigma^h(x) = p(x)\beta(\tilde{x}) \qquad (4)$$

where $p(x)$ are complete basis functions in the spatial coordinates x, which satisfy equilibrium in the domain and meet traction conditions on the local boundaries. The coefficients $\beta(\tilde{x})$ are also functions of x and are obtained by minimizing the following weighted L_2 norm:

$$J(\beta) = \sum_I^n w(\tilde{x} - x_I)[\,p(x_I)\beta(\tilde{x}) - \hat{\sigma}_I\,]^T[\,p(x_I)\beta(\tilde{x}) - \hat{\sigma}_I\,] \qquad (5)$$

where n is the number of points in the domain of influence (DOI) of $\tilde{x}$ for which the weight function $w(\tilde{x} - x_I) \neq 0$, and $\hat{\sigma}_I$ is the value of $\sigma(x)$ at sampling point (e.g. quadrature point) $x = x_I$. The statically admissible basis functions of stress components are normally coupled. Therefore the recovery is implemented for the whole stress vector instead of each component individually.

The weight function used in the current study is a fourth order spline function

$$w(\tilde{x} - x_I) = \begin{cases} 1 - 6(d_i/r_i)^2 + 8(d_i/r_i)^3 - 3(d_i/r_i)^4 & 0 \le d_i \le r_i \\ 0 & d_i \ge r_i \end{cases} \qquad (6)$$

in which $d_i = |\tilde{x} - x_I|$ is the distance from node x_I to point $\tilde{x}$. The symbol r_i is the radius of the DOI. Detailed information for implementing the MLS technique can be found in the literature.

A single edge cracked plate under end shearing (SECPS) studied by Xiao and Karihaloo [14] is shown in Fig. 6. A state of plane stress is considered and the thickness is assumed to be unity. All nodes on the bottom line (y = -8m) are fixed both in x- and y-directions. The PS element [13] is used. Stresses at 2×2 quadrature points are used in the SAR. Nodal stresses on the circle with radius r = 0.5 surrounding the crack tip (Fig. 6b) are compared in Fig. 7. The nodal stresses from the PS element are obtained directly from its trial stresses. The stresses corresponding to the first 15 terms (of each mode) of the Williams expansion obtained by Xiao et al. [3] using a 17-node HCE are also included as highly accurate reference solutions. The radius r_i of the DOI used by MLS is: r_i = 0.35 for the two nodes adjacent to the crack faces, and r_i = 0.2 for other points; r_i for nodes inside the domain is chosen close to the smallest side (diagonal) of surrounding elements. Thus, there are 8 – 11 quadrature points in the DOI of each point.

(a) (b)

$c = 3.5m$
$w = 7m$
$h = 8m$
$\tau = 1\ N/m^2$
$E = 10^5\ N/m^2$
$\nu = 0.25$

Fig. 6. (a) Geometry and loading conditions for the SECPS; (b) FE mesh with 96 quadrilateral elements giving 115 nodes.

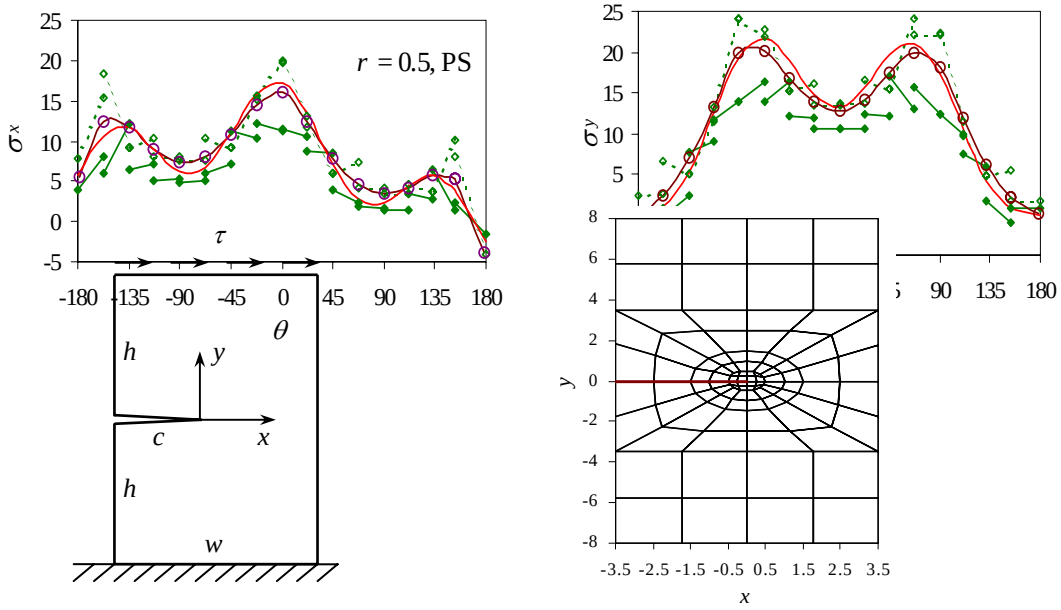

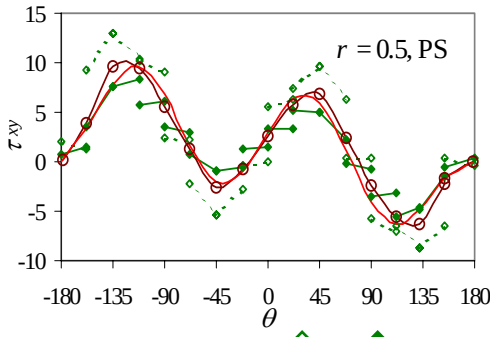

Fig. 7. Angular stress distributions along the circle $r = 0.5$. In the SAR, a linearly complete self-equilibriated stress field with 7 βs is used for all nodes in elements not adjacent to the traction-free boundary; a second order statically admissible stress field is used for nodes inside elements adjacent to the boundary (6 βs for one traction-free side; 5 βs for two adjacent traction-free sides).

In Fig. 7, a line segment ◇- - (-◆-) represents stresses within an element inside (outside) the circle; a line segment -○- represents the recovered stresses; —represents HCE results. These results demonstrate that the improvement after using the SAR is very promising.

5. FE FOR MODELLING THE POINT LOAD

In the Cartesian coordinate system shown in Fig. 8, the displacements in the neighbourhood of the point load are

$$\begin{Bmatrix} u_x \\ v_y \end{Bmatrix} = \begin{bmatrix} (1+\nu)\sin\theta\cos\theta & -(1-\nu)\theta \\ -(1+\nu)\sin^2\theta & -2\ln r \end{bmatrix} \frac{P}{\pi E} + \begin{Bmatrix} 1 \\ 0 \end{Bmatrix} A + \begin{Bmatrix} 0 \\ 1 \end{Bmatrix} B + \begin{Bmatrix} r\cos\theta \\ -r\sin\theta \end{Bmatrix} C \tag{7}$$

where *A*, *B*, and *C* are constants depending on the remote boundary conditions. Since the strain energy is unbounded in the neighbourhood of the point load, the above known deformation fields (7) cannot be used to enrich the general FE approximation via most methods appropriate for corners or crack tips. For example, if the PUM is used, the entries in the system stiffness matrix corresponding to the singular fields above will be very large (akin to penalty function terms). As a result the corresponding coefficient $P/(\pi E)$, if it is treated as an unknown variable, will vanish. The results cannot be improved even when the known amplitude $P/(\pi E)$ is enforced as a prescribed displacement. The DtN method extended by Seweryn [15] seems most appropriate for point loads. However, a required transformation to the system stiffness matrix will change the total degrees of freedom of the system. This has been avoided with the use of the penalty function approach [11].

The nodal displacement vector of the discrete system is expanded to include the coefficients in the displacement fields (7) of the neighbourhood of a point load. The known amplitude $P/(\pi E)$ is also treated as an unknown coefficient in the beginning, and later enforced as a prescribed displacement. The displacement field (7) acts as constraints on the displacements at nodes surrounding the loading point in the expanded unknown displacement vector. These constraints are enforced through a penalty function approach. Note that integration of singular integrands is avoided as no singular functions are used explicitly in the FE formulation. If the first ring of nodes surrounding the loading point is considered, a penalty factor of 10^3E guarantees convergence of numerical solutions.

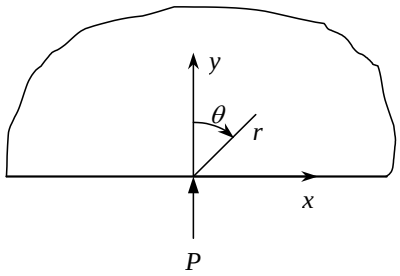

Fig. 8. A concentrated vertical force *P* per unit thickness acting on a horizontal straight boundary of an infinite plate.

6. A COMPRESSED SPARSE ROW (CSR) STORAGE SCHEME

A CSR storage scheme is introduced [12] since the widely used band storage schemes for the system stiffness matrix in a FE analysis can become less efficient with the use of the above techniques. Moreover, the discrete system of equations can be ill-conditioned after the enrichment, special solvers such as the HSL MA57 package may need to be used. This package requires that both the row and column indices of each non-zero element be stored together with its value.

As an example, the 6×6 symmetric sparse matrix *A* shown in Fig. 9 (*n*=6) is stored in CSR format in Table 3. (*val*(*ii*); *irn*(*ii*), *jcn*(*ii*)) store the triple (a_{ij}; *i*; *j*) for each non-zero entry in *A*; *kdg* stores the addresses of the diagonal entries of *A* in *val* to

$$\begin{bmatrix} a_{11} & a_{12} & & & & a_{16} \\ a_{21} & a_{22} & a_{23} & & & a_{26} \\ & a_{32} & a_{33} & a_{34} & a_{35} & \\ & & a_{43} & a_{44} & & \\ & & a_{53} & & a_{55} & a_{56} \\ a_{61} & a_{62} & & & a_{65} & a_{66} \end{bmatrix}$$

Fig. 9. A 6×6 symmetric sparse matrix.

simplify the retrieval of a specific element. *kdg*(*n*+1)=number of non-zero elements in *A*.

Table 3. Storage of the sparse matrix in Fig. 9.

val	a_{11}	a_{12}	a_{16}	a_{22}	a_{23}	a_{26}	a_{33}	a_{34}	a_{35}	a_{44}	a_{55}	a_{56}	a_{66}
irn	1	1	1	2	2	2	3	3	3	4	5	5	6
jcn	1	2	6	2	3	6	3	4	5	4	5	6	6
kdg	1	4	7	10	11	13							

The key point in the implementation of the CSR scheme is to analyze the profile, or locations of the non-zero entries, of the system stiffness matrix. This can be done in the following steps:

- For each node find its surrounding elements;
- For each node find the neighbouring nodes in the surrounding elements whose node numbers are larger than that of this node;
- Calculate the total number of non-zero entries;
- Analyze the sparsity profile of the system stiffness matrix, and calculate vectors *irn*, *jcn*, and *kdg*.

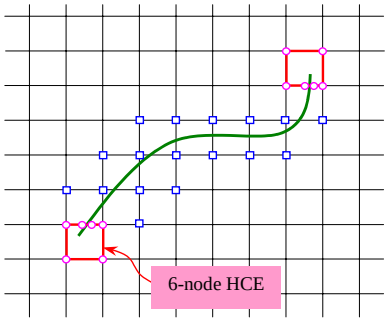

Fig. 10. A crack on a uniform mesh. The squared nodes are enriched by jump function as in XFEM but the crack tip zone is modelled by HCE. The two nodes where the crack cuts the side of a pre-existing quadrilateral element may be treated as virtual nodes or enriched by jump function.

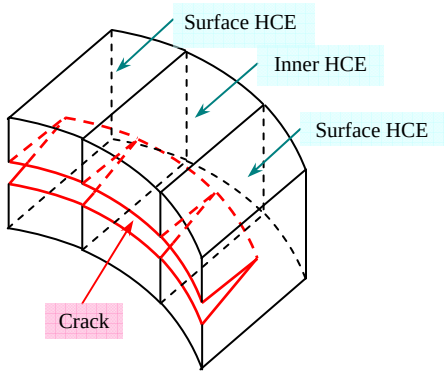

Fig. 11. Illustrative implementation of the HCE to a 3D crack problem. In the surface zone, the crack front intersects the traction free surface and the asymptotic expansion is different with that of the inner part. The HCE provides a seamless link between these asymptotic expansions.

7. FUTURE DEVELOPMENTS

- When the crack tip asymptotic field is available, HCE gives the most accurate crack tip fields. If it is used to model the crack tip region, and the XFEM is used for crack faces behind the crack tip (Fig. 10), the coupled method will retain advantages of both HCE and XFEM in 2-D and 3-D applications. Figure 11 illustrates the implementation of the HCE on a 3D crack.
- When the asymptotic crack field is not available, XFEM will be used together with the SAR. This coupled method simplifies the modelling of cracks, and predicts highly accurate crack tip fields.

REFERENCES

[1] Tong P, Pian THH, Lasry SJ. A hybrid element approach to crack problems in plane elasticity. *Int J Numer Meth Eng* 1973; 7: 297-308.

[2] Karihaloo BL, Xiao QZ. Accurate determination of the coefficients of elastic crack tip asymptotic field by a hybrid crack element with *p*-adaptivity. *Eng Fract Mech* 2001; 68: 1609-30.

[3] Xiao QZ, Karihaloo BL, Liu XY. Direct determination of SIF and higher order terms of mixed mode cracks by a hybrid crack element. *Int J Fract* 2004; 125: 207-25.

[4] Karihaloo BL, Xiao QZ. Implementation of HCE on a general FE mesh for interacting multiple cracks. *Proc ECCOMAS 2004*, Jyväskylä, Finland, 24 - 28 July, 2004.

[5] Daux C, Moes N, Dolbow J, Sukumar N, Belytschko T. Arbitrary branched and intersecting cracks with the extended finite element method. *Int J Numer Meth Eng* 2000; 48: 1741-60.

[6] Strouboulis T, Copps K, Babuska I. The generalized finite element method. *Comput Meth Appl Mech Eng* 2001; 190: 4081-193.

[7] Karihaloo BL, Xiao QZ. Modelling of stationary and growing cracks in FE framework without remeshing: a state-of-the-art review. *Comput Struct* 2003; 81: 119-29.

[8] Xiao QZ, Karihaloo BL. Direct evaluation of accurate coefficients of the linear elastic crack tip asymptotic field. *Fatig Fract Eng Mater Struct* 2003; 26: 719-30.

[9] Liu XY, Xiao QZ, Karihaloo BL. XFEM for direct evaluation of mixed mode SIFs in homogeneous and bi-materials. *Int J Numer Meth Eng* 2004; 59: 1103-18.

[10] Xiao QZ, Karihaloo BL. Statically admissible stress recovery using moving least squares technique. In: Topping BHV, Mota Soares CA, editors. Progress in Computational Structures Technology. Saxe-Coburg Publications, 2004.

[11] Xiao QZ, Karihaloo BL. FEM for evaluation of weight functions for SIF, COD and higher order coefficients with application to a typical wedge splitting specimen. *Int J Fract* 2004; 127: 201-37.

[12] Xiao QZ, Karihaloo BL. Implementation of a compressed sparse row storage scheme in FEM. Submitted to *Adv Eng Softw*, 2004.

[13] Pian THH, Sumihara K. Rational approach for assumed stress finite elements. *Int J Numer Meth Engng* 1984; 20; 1685-95.

[14] Xiao QZ, Karihaloo BL. Statically admissible stress recovery for crack problems. To be presented at, and to appear in the *Proc ICF*11, Turin, Italy, March, 2005.

[15] Seweryn A. Modeling of singular stress fields using finite element method. *Int J Solids Struct* 2002; 39: 4787–804.